ACS Macro Letters

Letter

pubs.acs.org/macroletters

Strongly Phase-Segregating Block Copolymers with Sub-20 nm Features

Kristian Kempe,[†,‡,∥,+] Kato L. Killops,[⊥] Justin E. Poelma,[∥] Hyunjung Jung,[#] Joona Bang,[#] Richard Hoogenboom,[▽] Helen Tran,[○] Craig J. Hawker,*[,∥,¶] Ulrich S. Schubert,*[,†,‡,◆] and Luis M. Campos*[,○]

[†]Laboratory of Organic and Macromolecular Chemistry (IOMC), Friedrich-Schiller-Universität Jena, Humboldtstr. 10, 07743 Jena, Germany

[‡]Jena Center for Soft Matter (JCSM), Friedrich-Schiller-Universität Jena, Philosophenweg 7, 07743 Jena, Germany

[∥]Materials Research Laboratory, Materials Department, and Department of Chemistry & Biochemistry, University of California, Santa Barbara, California 93016, United States

[⊥]Edgewood Chemical Biological Center, Aberdeen Proving Ground, Maryland 21010, United States

[#]Department of Chemical and Biological Engineering, Korea University, 136-713 Seoul, Republic of Korea

[▽]Supramolecular Chemistry Group, Department of Organic Chemistry, Ghent University, Krijgslaan 281 S4, B-9000 Ghent, Belgium

[○]Department of Chemistry, Columbia University, New York, New York 10027, United States

[◆]Dutch Polymer Institute (DPI), John F. Kennedylaan 2, 5612 AB Eindhoven, The Netherlands

[¶]Visiting Chair Professor at King Fahd University of Petroleum and Minerals, Dhahran, Saudi Arabia 31261

Supporting Information

ABSTRACT: The modular synthesis and lithographic potential of diblock copolymers based on polystyrene-*block*-poly(2-ethyl-2-oxazoline) (PS-*b*-PEtOx) are highlighted herein. Controlled radical and living cationic polymerization techniques were utilized to synthesize hydrophobic PS and hydrophilic PEtOx building block of varying molar mass. Subsequently, "click" chemistry was used to couple the blocks and obtain a family of PS-*b*-PEtOx polymers. The influence of molar mass, composition, and thin-film thickness on the microphase-segregated morphology and orientation were investigated with atomic force microscopy (AFM) and grazing incidence small-angle X-ray scattering (GISAXS). Dense hexagonal arrays of cylindrical nanodomains normal to the substrate, having a periodicity of less than 20 nm were obtained.

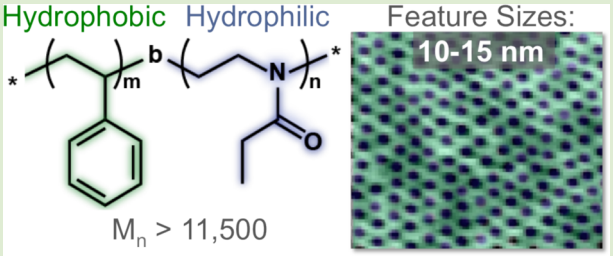

The microelectronics industry has driven advancements in nanopatterning strategies to obtain high-density devices, which continue to have a tremendous impact on information technology, communications, and health care. Top-down approaches have traditionally been the method of choice; however, bottom-up strategies offer many advantages, especially for accessing nanoscale features.[1−5] Block copolymers (BCPs) can be designed to phase-segregate under various conditions, including external stimuli such as electric or magnetic fields, or be guided epitaxially to obtain long-range order and complex patterns.[6−11] The modularity of these systems can be further exploited through orthogonal chemical modifications and controlled polymerization techniques to enhance phase segregation, tune the morphology, and introduce functionality.[9,12−15] The phase-separated domains obtained by BCP self-assembly are directly related to the size of the polymer (degree of polymerization, N), which can be controlled during the synthesis of the respective blocks. Along this vein, the phase segregation of the blocks depends on the Flory−Huggins interaction parameter (χ), which can be optimized by increasing the molar mass of each block or by changing the chemical composition of the blocks to maximize their repulsion energy.[16] For microphase separation to occur, the product of N and χ must be larger than a critical value. BCP self-assembly has enabled access to features with domain spacing (d-spacing) within the range of 15−200 nm.[6,17,18] Reducing the feature sizes accessible to BCP lithography is of particular interest for lithographic applications. However the challenge is that high molar mass BCPs generally lead to features having a d-spacing >30 nm, while low molar mass BCPs tend to become miscible, particularly when the volume fractions are mismatched. Recently, Ellison, Willson, and co-workers developed a novel strategy to align low molar mass BCPs with high repulsion

Received: June 13, 2013
Accepted: July 16, 2013
Published: July 19, 2013

   dx.doi.org/10.1021/mz400309d | *ACS Macro Lett.* 2013, 2, 677−682

interactions, which tend to preferentially orient along a given interface,[19] by using a top coat to neutralize the top interface and to induce perpendicular order leading to sub-10 nm features.[20] The success of this strategy provides added incentive for developing new materials with strongly phase-segregating domains that avoid the use of neutralization layers to obtain BCPs that maintain segregation at low molar masses for high-density arrays with sub-10 nm features.

To date, the most widely known BCPs having strong phase-segregation interactions are polystyrene-*b*-poly(4-vinylpyridine) (PS-*b*-P4VP) and polystyrene-*b*-polydimethylsiloxane (PS-*b*-PDMS), in addition to triblock copolymers of polylactide and PDMS.[8,21,22] Since the driving force for phase segregation in polystyrene-*b*-poly(ethylene oxide) (PS-*b*-PEO) is less than the systems above, we have previously found that changing the architecture from linear to cyclic PS-*b*-PEO can yield cylindrical morphologies with *d*-spacing ca. 19.5 nm by solvent annealing.[23] However, these cyclic polymers are difficult to synthesize in large scale. Given the limited access to strongly phase-segregating BCPs and the need to reliably obtain dense arrays exhibiting sub-20 nm resolution, a new materials system based on BCPs composed of PS and a hydrophilic block derived from poly(2-oxazoline) (POx) is described herein.

Since the development of cationic ring-opening polymerization (CROP) of 2-oxazolines in 1966,[24−27] prohibitively long reaction times have precluded the widespread adoption of POx derivatives as building blocks for a wide range of polymeric systems. In the past decade, studies involving POx have experienced a resurgence due to the significant acceleration of polymerization times from days to minutes through microwave irradiation.[28−30] Furthermore, the living character of these microwave-accelerated polymerizations enables a high degree of control over end-group functionality through the exploitation of functional initiators or via terminating agents and postpolymerization modifications.[31−35] Another attractive feature of POx polymers[36] is the structural versatility inherent through changing the substituent at the 2-position of the monomer which leads to materials exhibiting drastically different properties.[37−41] In particular, polymers of 2-methyl-2-oxazoline (MeOx) and 2-ethyl-2-oxazoline (EtOx) are of considerable interest due to their remarkably similar properties to PEO, especially with respect to biomedical applications.[42−44] Analogous to PEO, PMeOx and PEtOx are water-soluble and undergo strong phase separation from PS. However, unlike PEO, these polymers are not crystalline and are thus attractive for thin-film processing.

To probe the self-assembly behavior of PS-*b*-PEtOx, a family of BCPs was synthesized in a modular fashion by coupling azide end-functionalized PS and alkyne-terminated PEtOx through copper-catalyzed azide−alkyne cycloaddition (CuAAC) with different molar masses and volume fractions.[45,46] These materials were then examined as BCP templates for the fabrication of sub-20 nm features.

The initial synthetic challenge in this study was the development of a versatile and efficient procedure for the synthesis of PS-*b*-PEtOx diblock copolymers. Since each block requires different polymerization techniques which are non-trivial to execute sequentially, blocks of PS and PEtOx were prepared individually with functional azide and alkyne end groups, respectively, that can then be coupled via a CuAAC reaction (Scheme 1). Both controlled radical polymerization (CRP) and CROP techniques allow for the straightforward introduction of end group functionalities, a strategy that has been previously employed to yield architectural variations of polymers,[47,48] e.g., end group functionalized vinyl and oxazoline-based homopolymers.[49−51] Well-defined, chain-end functionalized PS derivatives were therefore synthesized by atom transfer radical polymerization (ATRP) followed by displacement of the bromide chain-end with sodium azide to yield the required azide-functional end group.[52,53] The PEtOx block was functionalized with a complementary alkyne by direct termination of the living cationic species with hexynoic acid leading to an ester linkage, thereby providing a potential degradable linker in contrast to initiation with propargyl tosylate.[34,54,55]

Scheme 1. Schematic Representation of the Polymerization Techniques Applied for the Synthesis of Individual Building Blocks and the CuAAC Reaction of the Corresponding End-Functionalized Blocks[a]

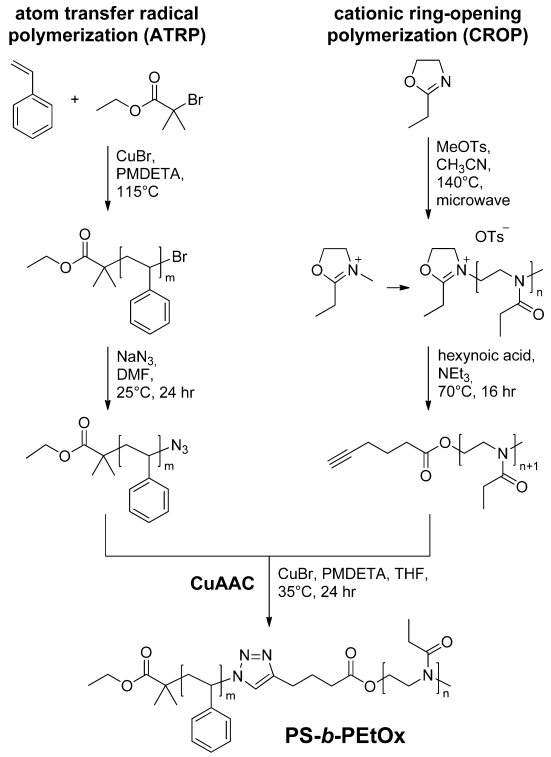

[a]PMDETA = *N*,*N*,*N*′,*N*″,*N*″-pentamethyldiethylenetriamine, NaN_3 = sodium azide, DMF = dimethylformamide, MeOTs = methyl tosylate, CH_3CN = acetonitrile, NEt_3 = triethylamine, THF = tetrahydrofuran.

To attain sub-20 nm features, low molecular weight PS-*b*-PEtOx BCPs were synthesized, as summarized in Table 1. Four

Table 1. Sample Characteristics of PS-*b*-PEtOx Diblock Copolymers

sample	molar mass$_{PEtOx}$ [g mol^{-1}]	molar mass$_{PS}$ [g mol^{-1}]	molar mass$_{total}$[a] [g mol^{-1}]	M_n[b] [g mol^{-1}]	PDI[b]	f_{PEtOx}[c]
BCP1	6000	13000	19000	17000	1.24	30
BCP2	4000	13000	17000	16000	1.18	22
BCP3	2000	13000	15000	14000	1.20	12
BCP4	2000	10000	12000	11500	1.10	16

[a]Theoretical; calculated based on the molar mass obtained for the individual building blocks. [b]Determined by SEC, eluent: $CHCl_3$. [c]Volume fraction (ρ_{PS} = 1.05 g cm^{-3}, ρ_{PEtOx} = 1.14 g cm^{-3}).[56]

dx.doi.org/10.1021/mz400309d | *ACS Macro Lett.* 2013, 2, 677−682

BCPs with varying molar mass were prepared with volume fractions of PEtOx ranging from 12 to 30%: **BCP1** (PS_{13k}-*b*-$PEtOx_{6k}$), **BCP2** (PS_{13k}-*b*-$PEtOx_{4k}$), **BCP3** (PS_{13k}-*b*-$PEtOx_{2k}$), and **BCP4** (PS_{10k}-*b*-$PEtOx_{2k}$). The efficiency of the CuAAC coupling and ease of purification by simple precipitation in cold methanol to remove the slight excess of PEtOx are evidenced by the monomodal shape of the size exclusion chromatography (SEC) traces and the narrow polydispersity index (PDI) values of the final BCPs (Figure 1). ^{1}H NMR spectroscopy analysis

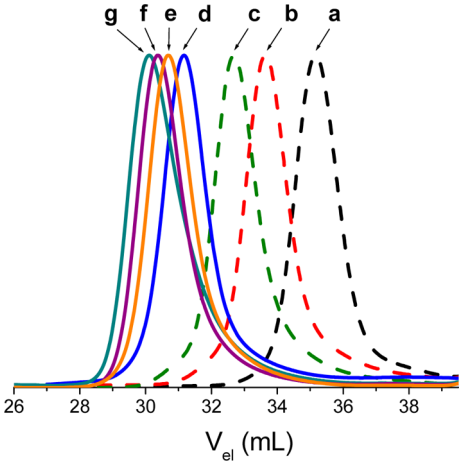

Figure 1. SEC traces of PEtOx obtained by microwave-assisted cationic ring-opening polymerization (a, $PEtOx_{2k}$; b, $PEtOx_{4k}$; c, $PEtOx_{6k}$) and the corresponding block copolymers after CuAAC coupling (d, **BCP4** (PS_{10k}-*b*-$PEtOx_{2k}$); e, **BCP3** (PS_{13k}-*b*-$PEtOx_{2k}$); f, **BCP2** (PS_{13k}-*b*-$PEtOx_{4k}$); g, **BCP1** (PS_{13k}-*b*-$PEtOx_{6k}$)).

illustrates the decreasing mole fraction of PEtOx relative to PS from **BCP1** to **BCP3** (Supporting Information, Figure S1), which correlates well with the SEC values (Table 1), further confirming the fidelity of this approach.

The thermal properties of **BCP1**–**BCP3** were investigated using differential scanning calorimetry (DSC) (Figure 2). For

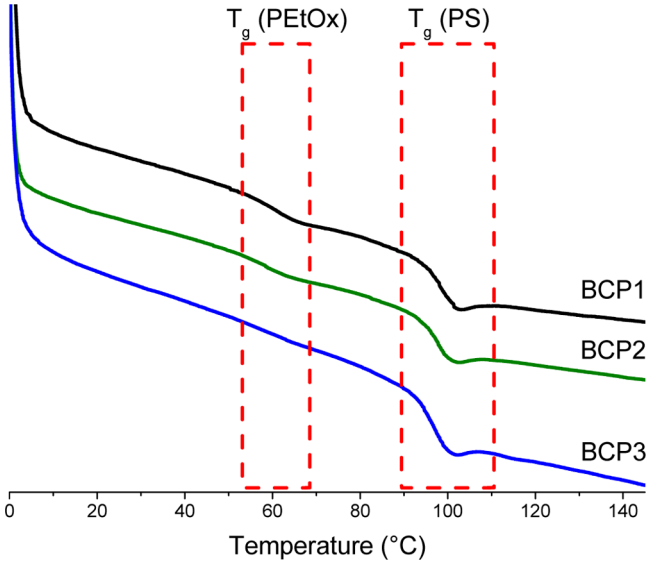

Figure 2. DSC curves of **BCP1** (PS_{13k}-*b*-$PEtOx_{6k}$), **BCP2** (PS_{13k}-*b*-$PEtOx_{4k}$), and **BCP3** (PS_{13k}-*b*-$PEtOx_{2k}$) demonstrating the presence of two glass transition temperatures, as outlined. The curves were obtained during the third heating run.

immiscible and partially miscible systems, two distinct glass transition temperatures (T_g) are expected. Here, all three BCPs exhibited two independent T_g values at ca. 60 °C and ca. 100 °C, which can be assigned to the individual blocks, PEtOx and PS, respectively. Notably, two T_g's were observed for **BCP3** which possesses the shortest PEtOx block and lowest volume fraction of PEtOx (2,000 g mol^{-1}, f_{PEtOx} = 12). With decreasing volume fraction of the PEtOx block, the corresponding T_g became less pronounced, while the higher volume fraction PS block was still clearly visible. In addition, none of the BCPs displayed any melting transition up to 140 °C, further confirming their amorphous character. Significantly, the presence of two T_g's for all the PS-*b*-PEtOx diblock copolymers supports strong segregation between the PEtOx and PS domains.

The thin-film surface morphologies of these systems were initially examined by atomic force microscopy (AFM). BCP solutions were first spin-cast onto silicon substrates with the as-cast films of all BCPs, **BCP1**–**4**, displaying featureless surfaces (Supporting Information, Figure S2a). The films were subsequently annealed at room temperature in a saturated toluene atmosphere and quenched in a high humidity chamber, at approximately 90% relative humidity. It should be noted that exposure of the films to ambient humidity was not sufficient to induce the formation of perpendicular structures (Supporting Information, Figure S2b), and this reliance on quenching at high humidity has been demonstrated to be crucial for the formation of highly ordered arrays of nanostructures normal to the substrate in PEO-based copolymers.[57] Considering that the hydrophilicity of PEtOx is comparable to PEO, observation of similar behavior for the PS-*b*-PEtOx systems is not surprising. AFM images of annealed films of **BCP1**–**BCP4** revealed ordered structures with ca. 20 nm *d*-spacings and sub-20 nm features (Figure 3, Table 2, and Figure S2, Supporting Information). Although hexagonally packed cylinders were observed after 12 h of solvent annealing for **BCP1**, defects diminished, and long-range ordering improved for thin films annealed for 24 h; however, prolonged annealing times (48 h) did not lead to any further increase in ordering. In each case, the thin-film morphology was also not affected by film thickness up to 200 nm.

To determine the influence of PEtOx volume fraction on microphase segregation, three BCPs with identical PS block length (13 000 g mol^{-1}) were compared under identical conditions. For **BCP1** and **BCP2**, nanoscopic domains of PEtOx, which appear darker in the AFM height image, embedded in a matrix of PS were evident from thin-film studies. In contrast, **BCP3** with a PEtOx volume fraction of 12% showed low contrast in the AFM images (Figure 3). Previously, the strong contrast of PS-*b*-PEO films was ascribed to surface dimples; i.e., the hydrophilic PEO domains were selectively swollen by water vapor, and then the PEO chains collapsed after evaporation of water.[49] Hence, the difference between **BCP1**/**BCP2** and **BCP3** results from a morphology change as the volume fraction of PEtOx decreases with **BCP3** forming spheres rather than cylinders. Assuming that arrays of hemispheres were formed at the surface, the chain collapse would be less pronounced than cylindrical structures due to the geometric confinement of hemispheres, leading to the lower contrast observed for **BCP3** when compared to **BCP1**/**BCP2** (cylindrical morphology). This rationale is further reinforced by **BCP4**, which was designed to have a shorter PS block (10 000 g mol^{-1}) while maintaining the identical PEtOx block (2000 g

dx.doi.org/10.1021/mz400309d | *ACS Macro Lett.* 2013, 2, 677–682

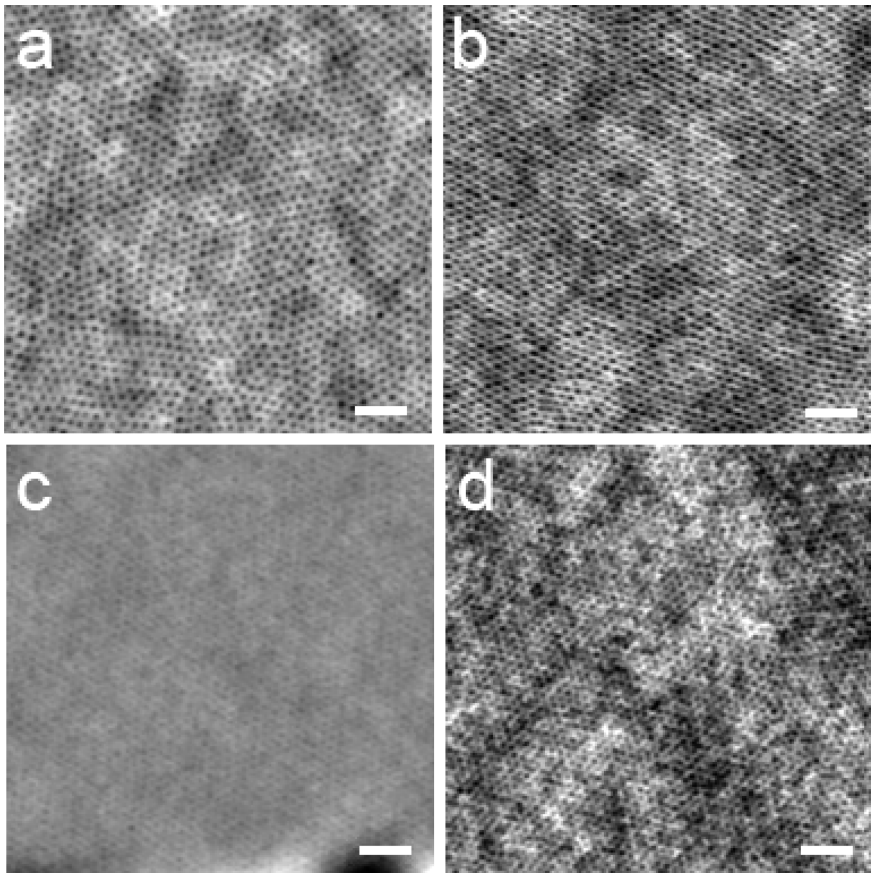

Figure 3. Representative AFM height images of the thin films (80 nm) of **BCP1** (a), **BCP2** (b), **BCP3** (c), and **BCP4** (d) upon annealing in saturated toluene vapor for 24 h. Scale bar = 100 nm.

Table 2. Characteristics of the Thin Films Determined by AFM and GISAXS

sample	M_{total}[a] [g mol^{-1}]	f_{PEtOx}[b]	*d*-spacing[c] [nm]	*d*-spacing[d] [nm]	feature size[c] [nm]	morphology and orientation[c,d]
BCP1	19000	30	22.4	21.5	13.5 ± 0.9	cylinders
BCP2	17000	22	19.6	19.1	14.6 ± 1.4	cylinders
BCP3	15000	12	18.4	19.7	12.7 ± 1.4	spheres
BCP4	12000	16	17.6	18	10.4 ± 0.9	cylinders

[a]Theoretical molar mass; calculated based on the molar mass obtained for the individual building blocks. [b]Volume fraction (ρ_{PS} = 1.05 g cm^{-3}, ρ_{PEtOx} = 1.14 g cm^{-3}).[56] [c]Determined by AFM. [d]Determined by GISAXS (all cylinders are orthogonal to the substrate).

mol^{-1}) as **BCP3**. This leads to a PEtOx volume fraction of 16% for **BCP4**, and the ability to use the same starting PEtOx block allows the effect of the PS block length on morphology to be studied directly. Similar to **BCP1** and **BCP2**, AFM images of the thin films of **BCP4** revealed the formation of highly ordered hexagonally packed cylinders normal to the substrate with the *d*-spacing of these cylinders being varied in accord to volume fraction and composition of each block (Table 2).

To more accurately characterize the morphology, *d*-spacing, and orientation, the annealed thin films were evaluated by grazing-incidence small-angle X-ray scattering (GISAXS), which was carried out at the 9A beamline at the Pohang Accelerator Laboratory (PAL), Korea. First, the requisite of quenching at high humidity conditions was confirmed. 2D scattering results for **BCP1** at ambient humidity revealed both the presence of first scattering peaks and disordered rings, whereas exclusively Bragg's rods appeared under high humidity conditions (Supporting Information, Figure S3). These results are in full agreement with the AFM analysis. For **BCP1**, **BCP2**, and **BCP4**, the sharp Bragg q_{xy} rods along the q_z direction of thin films is indicative of hexagonal packing of cylindrical microdomains oriented normal to the film surface (Supporting Information, Figure S4). For **BCP3**, it was found that the scattering intensity was significantly lower than other samples. This can be attributed to less surface dimples, as we note that **BCP3** contains only 12% volume fraction of PEtOx, which is more likely to exhibit a spherical morphology as deduced from the AFM images. According to in-plane scattering analysis, the first-order peaks were located at q_{xy} = 0.304 nm^{-1} (**BCP1**), 0.328 nm^{-1} (**BCP2**), 0.319 nm^{-1} (**BCP3**), and 0.347 nm^{-1} (**BCP4**) along the q_z direction. Determined by Bragg's law, the *d*-spacings of the BCPs are 21.5 nm (**BCP1**), 19.1 nm (**BCP2**), 19.7 nm (**BCP3**), and 18 nm (**BCP4**), which are in good agreement with the values obtained by AFM (Table 2). Due to the presence of higher-order scattering peaks, the annealed polymer thin films were assigned hexagonally packed structures. It should be noted that this behavior is analogous to PS-*b*-PEO systems with similar volume fractions of the PEO block, albeit with smaller feature sizes.

dx.doi.org/10.1021/mz400309d | *ACS Macro Lett.* 2013, 2, 677−682

PEtOx has been shown to be a versatile domain component for BCP lithography. The ease of synthesis, lack of crystallinity, and strong phase segregation allow for the fabrication of ordered thin films with tunable sub-20 nm feature sizes and sub-20 nm periodicity. A family of PS-*b*-PEtOx BCPs with varying total molar mass and volume fractions of PEtOx, representing the minor component, could be readily prepared using a modular "click" approach. AFM and GISAXS measurements revealed a strong dependency of the morphology on the PEtOx volume fraction. Analogous to PS-*b*-PEO, annealed thin films displayed hexagonally packed cylindrical microdomains oriented perpendicular to the surface without prior neutralization of the surface or incorporation of a labile linker between both blocks. However, unlike PS-*b*-PEO, smaller feature sizes could be accessed since phase segregation at low molecular masses is maintained due to the increased repulsion energy between the blocks.

■ ASSOCIATED CONTENT

Ⓢ Supporting Information

Experimental details, Table S1, and Figures S1−S4. This material is available free of charge via the Internet at http://pubs.acs.org.

■ AUTHOR INFORMATION

Corresponding Author

*E-mail: lcampos@columbia.edu.

Present Address

[+]Nanostructured Interfaces and Materials Group, Department of Chemical & Biomolecular Engineering, The University of Melbourne, Parkville, Victoria 3010, Australia.

Notes

The authors declare no competing financial interest.

■ ACKNOWLEDGMENTS

This material is based upon work supported by the National Science Foundation (MRSEC Program − DMR-1121053, K.K., J.E.P., C.J.H). This work was also partially supported by the Institute for Collaborative Biotechnologies through contract number W911NF-09-D-0001 from the US Army Research Office (K.L.K., C.J.H.) and the Surface Science Initiative under the US Army Basic Research Program (W911NH-12-1-0252) (K.L.K. and L.M.C.). K.K. is grateful to the Landesgraduierten-foerderung Thueringen and the German Academic Exchange Service (DAAD) for financial support. J.E.P. thanks NSF GRFP for funding. R.H. acknowledges the Ghent University for support via the Concerted Research Actions (project BOF11/GOA/023). U.S.S. thanks the Dutch Polymer Institute (DPI, Technology area HTE) and the Freistaat Thüringen for financial support. H.T. thanks the Department of Defense (DoD) for a National Defense Science & Engineering Graduate (NDSEG) Fellowship. H.J. and J.B. acknowledge the support by Nano Material Technology Development Program through the National Research Foundation funded by the Korean Government (MOEHRD) (2012M3A7B4049863) and the Human Resources Development Program of KETEP grant (No. 20114010203050).

■ REFERENCES

(1) Hamley, I. W. *Angew. Chem., Int. Ed.* **2003**, *42*, 1692.
(2) Hamley, I. W. *Block Copolymers in Solution: Fundamentals and Applications.*; John Wiley & Sons Ltd: Chichester, England, 2005.
(3) Gohy, J.-F. *Adv. Polym. Sci.* **2005**, *190*, 65.
(4) Tran, H.; Killops, K. L.; Campos, L. M. *Soft Matter* **2013**, *9*, 6578.
(5) Zhong, X.; Bailey, N. A.; Schesing, K. B.; Bian, S.; Campos, L. M.; Braunschweig, A. B. *J. Polym. Chem., Part A: Polym. Chem.* **2013**, *51*, 1533.
(6) Bang, J.; Jeong, U.; Ryu, D. Y.; Russell, T. P.; Hawker, C. J. *Adv. Mater.* **2009**, *21*, 4769.
(7) Yang, J. K. W.; Jung, Y. S.; Chang, J. B.; Mickiewicz, R. A.; Alexander-Katz, A.; Ross, C. A.; Berggren, K. K. *Nat. Nanotechnol.* **2010**, *5*, 256.
(8) Bita, I.; Yang, J. K. W.; Jung, Y. S.; Ross, C. A.; Thomas, E. L.; Berggren, K. K. *Science* **2008**, *321*, 939.
(9) Tang, C.; Lennon, E. M.; Fredrickson, G. H.; Kramer, E. J.; Hawker, C. J. *Science* **2008**, *322*, 429.
(10) Thurn-Albrecht, T.; DeRouchey, J.; Russell, T. P.; Jaeger, H. M. *Macromolecules* **2000**, *33*, 3250.
(11) Tran, H.; Gopinadhan, M.; Majewski, P. W.; Shade, R.; Steffes, V.; Osuji, C. O.; Campos, L. M. *ACS Nano* **2013**, *7*, 5514.
(12) Killops, K. L.; Gupta, N.; Dimitriou, M. D.; Lynd, N. A.; Jung, H.; Tran, H.; Bang, J.; Campos, L. M. *ACS Macro Lett.* **2012**, *1*, 758.
(13) Rao, J.; De, S.; Khan, A. *Chem. Commun.* **2012**, *48*, 3350.
(14) Kuan, W.-F.; Roy, R.; Rong, L.; Hsiao, B. S.; Epps, T. H. *ACS Macro Lett.* **2012**, *1*, 519.
(15) Barner-Kowollik, C.; Du Prez, F. E.; Espeel, P.; Hawker, C. J.; Junkers, T.; Schlaad, H.; Van Camp, W. *Angew. Chem., Int. Ed.* **2011**, *50*, 60.
(16) Bates, F.; Fredrickson, G. *Annu. Rev. Phys. Chem.* **1990**, *41*, 525.
(17) Xia, Y.; Olsen, B. D.; Kornfield, J. A.; Grubbs, R. H. *J. Am. Chem. Soc.* **2009**, *131*, 18525.
(18) Rzayev, J. *ACS Macro Lett.* **2012**, *1*, 1146.
(19) Ryu, D. Y.; Shin, K.; Drockenmuller, E.; Hawker, C. J.; Russell, T. P. *Science* **2005**, *308*, 236.
(20) Bates, C. M.; Seshimo, T.; Maher, M. J.; Durand, W. J.; Cushen, J. D.; Dean, L. M.; Blachut, G.; Ellison, C. J.; Willson, C. G. *Science* **2012**, *338*, 775.
(21) Jeong, U. Y.; Kim, H. C.; Rodriguez, R. L.; Tsai, I. Y.; Stafford, C. M.; Kim, J. K.; Hawker, C. J.; Russell, T. P. *Adv. Mater.* **2002**, *14*, 274.
(22) Rodwogin, M. D.; Spanjers, C. S.; Leighton, C.; Hillmyer, M. A. *ACS Nano* **2010**, *4*, 725.
(23) Poelma, J. E.; Ono, K.; Miyajima, D.; Aida, T.; Satoh, K.; Hawker, C. J. *ACS Nano* **2012**, *6*, 10845.
(24) Bassiri, T. G.; Levy, A.; Litt, M. *J. Polym. Sci., Part C: Polym. Lett.* **1967**, *5*, 871.
(25) Kagiya, T.; Narisawa, S.; Maeda, T.; Fukui, K. *J. Polym. Sci., Part C: Polym. Lett.* **1966**, *4*, 441.
(26) Seeliger, W.; Aufderhaar, E.; Diepers, W.; Feinauer, R.; Nehring, R.; Thier, W.; Hellmann, H. *Angew. Chem., Int. Ed.* **1966**, *5*, 875.
(27) Tomalia, D. A.; Sheetz, D. P. *J. Polym. Sci., Part A: Polym. Chem.* **1966**, *4*, 2253.
(28) Ebner, C.; Bodner, T.; Stelzer, F.; Wiesbrock, F. *Macromol. Rapid Commun.* **2011**, *32*, 254.
(29) Kempe, K.; Becer, C. R.; Schubert, U. S. *Macromolecules* **2011**, *44*, 5825.
(30) Wiesbrock, F.; Hoogenboom, R.; Leenen, M. A. M.; Meier, M. A. R.; Schubert, U. S. *Macromolecules* **2005**, *38*, 5025.
(31) Kempe, K.; Hoogenboom, R.; Jaeger, M.; Schubert, U. S. *Macromolecules* **2011**, *44*, 6424.
(32) Manzenrieder, F.; Luxenhofer, R.; Retzlaff, M.; Jordan, R.; Finn, M. G. *Angew. Chem., Int. Ed.* **2011**, *50*, 2601.
(33) Volet, G. l.; Lav, T.-X.; Babinot, J.; Amiel, C. *Macromol. Chem. Phys.* **2011**, *212*, 118.
(34) Fijten, M. W. M.; Haensch, C.; van Lankvelt, B. M.; Hoogenboom, R.; Schubert, U. S. *Macromol. Chem. Phys.* **2008**, *209*, 1887.
(35) Guillerm, B.; Monge, S.; Lapinte, V.; Robin, J. J. *Macromol. Rapid Commun.* **2012**, *33*, 1600.
(36) Hoogenboom, R. *Angew. Chem., Int. Ed.* **2009**, *48*, 7978.

(37) Kempe, K.; Lobert, M.; Hoogenboom, R.; Schubert, U. S. *J. Polym. Sci., Part A: Polym. Chem.* **2009**, *47*, 3829.
(38) Makino, A.; Kobayashi, S. *J. Polym. Sci., Part A: Polym. Chem.* **2010**, *48*, 1251.
(39) Kobayashi, S.; Uyama, H. *J. Polym. Sci., Part A: Polym. Chem.* **2002**, *40*, 192.
(40) Aoi, K.; Okada, M. *Prog. Polym. Sci.* **1996**, *21*, 151.
(41) Kempe, K.; Jacobs, S.; Lambermont-Thijs, H. M. L.; Fijten, M. M. W. M.; Hoogenboom, R.; Schubert, U. S. *Macromolecules* **2010**, *43*, 4098.
(42) Adams, N.; Schubert, U. S. *Adv. Drug Delivery Rev.* **2007**, *59*, 1504.
(43) Bauer, M.; Lautenschlaeger, C.; Kempe, K.; Tauhardt, L.; Schubert, U. S.; Fischer, D. *Macromol. Biosci.* **2012**, *12*, 986.
(44) Satoh, K.; Poelma, J. E.; Campos, L. M.; Stahl, B.; Hawker, C. J. *Polym. Chem.* **2012**, *3*, 1890.
(45) Rostovtsev, V. V.; Green, L. G.; Fokin, V. V.; Sharpless, K. B. *Angew. Chem., Int. Ed.* **2002**, *41*, 2596.
(46) Tornøe, C. W.; Christensen, C.; Meldal, M. *J. Org. Chem.* **2002**, *67*, 3057.
(47) Kempe, K.; Krieg, A.; Becer, C. R.; Schubert, U. S. *Chem. Soc. Rev.* **2012**, *41*, 176.
(48) Fournier, D.; Hoogenboom, R.; Schubert, U. S. *Chem. Soc. Rev.* **2007**, *36*, 1369.
(49) Isaacman, M. J.; Barron, K. A.; Theogarajan, L. S. *J. Polym. Sci., Part A: Polym. Chem.* **2012**, *50*, 2319.
(50) Marx, L.; Volet, G.; Amiel, C. *J. Polym. Sci., Part A: Polym. Chem.* **2011**, *49*, 4785.
(51) Rayeroux, D.; Lapinte, V.; Lacroix-Desmazes, P. *J. Polym. Sci., Part A: Polym. Chem.* **2012**, *50*, 4589.
(52) Campos, L. M.; Killops, K. L.; Sakai, R.; Paulusse, J. M. J.; Damiron, D.; Drockenmuller, E.; Messmore, B. W.; Hawker, C. J. *Macromolecules* **2008**, *41*, 7063.
(53) Thibault, R. J.; Takizawa, K.; Lowenheilm, P.; Helms, B.; Mynar, J. L.; Frechet, J. M. J.; Hawker, C. J. *J. Am. Chem. Soc.* **2006**, *128*, 12084.
(54) Weber, C.; Becer, C. R.; Hoogenboom, R.; Schubert, U. S. *Macromolecules* **2009**, *42*, 2965.
(55) Miyamoto, M.; Naka, K.; Tokumizu, M.; Saegusa, T. *Macromolecules* **1989**, *22*, 1604.
(56) Brandrup, J.; Immergut, E. H.; Grulke, E. A.; Abe, A.; Bloch, D. R. *Polymer Handbook*, 4th ed.; John Wiley & Sons: New York, 1999, 2005.
(57) Bang, J.; Kim, B. J.; Stein, G. E.; Russell, T. P.; Li, X.; Wang, J.; Kramer, E. J.; Hawker, C. J. *Macromolecules* **2007**, *40*, 7019.